Analysing the acoustic performance of a nearly-enclosed noise barrier using scale model experiments and a 2.5-D BEM approach

Qiutong Li, Denis Duhamel, Yanyun Luo, Honore Yin

Analyzing acoustic performance of a nearly-enclosed noise barrier using scale experiments and a 2.5-D BEM approach

Qiutong Li, Denis Duhamel, Yanyun Luo, Honore Yin

Abstract

This paper describes scale modelling method to measure the acoustic performance of a nearly-enclosed barrier and corresponding predictions using an existing 2.5-D Boundary Element Method(BEM) program. Preliminary investigation results show the deterioration in performance of a nearly-enclosed barrier due to the resonance effect that led to high pressure levels radiating into the surroundings via the topped opening. Absorptive material added to the inner surface of the barrier can effectively improve this phenomenon. Measurements on one-twentieth scale model of barriers, viaducts and vehicle structures were carried out outdoors under controlled conditions. The measured results show the transmission loss of transparent panels on the top were not adequate to make the measured results as high as the predictions. A modified scale model, by coating all the surfaces with rubber, was remeasured. The results from retested tests and calculations were in good agreement each other, which indicate that the 2.5-D BEM code can provide a reliable description of the acoustic performance of a nearly-enclosed barrier. Then the program was able to be employed into the investigation of barrier performance on every area with different acoustic features in the surrounding environment. As expected, the attenuation of the nearly-enclosed barrier averaged around 15 dB in the near filed and around 10 dB in the far field. The number effect of incoherent point sources on the performance is discussed as well for the study of railway traffic noise. The increased number of incoherent point sources can result in smoother and lower attenuations for the whole sound field.

Keywords: Enclosed noise barrier, scale model measurement, BEM

1. Introduction

In general, noise barriers are built on the side of viaducts to reduce urban railway traffic noise pollution. The associated acoustic performance is thought to depend largely on their height and the relative distance between the source, the barrier and receiver positions[1]. There is almost no change for the latter since the predominant source for urban railway traffic is located on the place of wheel-rail interaction, and the barrier position, varying with changes of width of the viaduct, remains basically unchanged. To improve the performance devices installed on the top of the barrier are sometimes introduced instead of the height increase. Among all the barriers on the market, enclosed types are common solutions to improve the most. LI. et al.[2] studied on the noise reduction of semi- or fully-enclosed barriers of high speed railways using the full-scale modelling. The results showed that the attenuation of fully-enclosed metal noise barrier with composite sound absorption plates was up to 25 dB(A) at 7.5m distance from the track central line. However, the barrier cannot be fully-enclosed when consider the fire safety. Since the space inside an enclosed barrier is very small when a train passes by, an opening, commonly with a two-meter height, is designed on the top so that smoke can be emitted when fire occurs. In the present study this kind of barrier is called a nearly-enclosed barrier, one of the prototypes depicted in Figure 1. The two arched parts on the top are made of 6.5-mm-thick PC panels that allows in natural light and to reduce limitation of drivers' view[3]. One of the important issues is the sufficiency of the sound insulation property of such material that is required to achieve suitable acoustical performance.

Another for that is the multiple reflections between two axisymmetric parts and between the extremely high barrier and the vehicle surface that significantly degrade barrier performance. Watts[4] found a reflecting wall with a 2m height fixed on the source side could result in a reduction of 4 dB(A) in the insertion loss of a sound barrier of the same height. More seriously in our study, the acoustical domain bounded by a nearly-enclosed barrier can be considered as a room with a door or an open duct, and then the sound field within such domain can be dominated by acoustic resonance. Under the influence of this effect high pressure amplitudes may be observed at the resonant frequencies leading to the significant degradation of barrier performance. In the parametric investigation of the performance of multiple edge highway noise barriers, D.J. Oldham and C.A. Egan[5] observed the

acoustic resonance in the air in the gap between an edge and the barrier face resulting in the negative relative insertion loss for the configurations involving reflective edges located on the source side of the barrier. In parallel with this development, Yang et al.[6] firstly proposed the resonance effect of the trapped modes to explain the deterioration in performance of a conventional barrier due to the reflecting surface. To solve the multiple reflections and the peak sound pressures governed by resonance, a tilted barrier was proposed[7, 8] as a solution with a slope of ten degrees gaining the best profit and a wave-trapping barrier was proposed[6] effectively in reducing the deterioration at peak frequencies. Furthermore, absorptive materials were employed on the surface of reflective barrier near the source being able to reduce the deterioration with highly efficiency[9].

A number of studies have made clear the importance of "T", "Y" and other top devices in improving the diffraction reduction of barriers but there is little research as a specific guidance that can be applied to the problems discussed in this paper. Thus the objective of this research is to analyze acoustic performance of a nearly-enclosed barrier using numerical and experimental method. An existing 2.5-D BEM program was used to characterise the acoustic performance of a nearly-enclosed barrier on every area with different acoustic features in the surrounding environment. Its reliability was validated by comparing predictions with measured results from scale model tests. The scale modelling technique is more efficient and more accurate to not only investigate barrier performance, but also to realize the effect of related parameters on the acoustic performance. By using scale experiments and 2.5-D BEM approach the efficiency of noise reduction of constructed panels and the number effect of incoherent point source are also studied.

Section 1 of this paper briefly introduces a nearly-enclosed barrier commonly applied on the city viaduct railway traffic system and some relevant issues need to be resolved. Section 2 presents a 2.5-D BEM model obtained from a real prototype. The resonance effect of acoustic modes on barrier performance is also described by a preliminary investigation in this section. Section 3 validates the numerical model by a series of scale measurements. As a result of the measured results much lower than those predictions, the sound insulation property of transparent material is discussed in this section. Then a series of remeasurement on the modified model is described and the results give confidence in the subsequent predictions. Section 4 predicts acoustic performance of a nearly-enclosed barrier by using 2.5-D BEM modelling. The attenuation of barrier located at several receiver positions

in the near and far field comparing different source types are discussed in detail, and all the predicted results are summarized. Section 5 gives a brief conclusion in this paper.

2. 2.5-D Boundary element modelling

Based on the direct formulation of Boundary Element Method(BEM), the 2-D, 2.5-D and 3-D BEM numerical methods were developed and detailed in [10–15]. In the 2-D numerical simulation, a 2-D point source is commonly approximated as an infinite coherent line source in three dimensions; the barrier and other obstacles are defined with the cross-section remaining constant and infinite along a direction perpendicular to the section plane. 2.5-D BEM method gives a chance to allow the use of other sources like a point source or an incoherent line source but remain the geometrical characteristics of all the obstacles. DUHAMEL[14] compared these three source types and figured out that the results predicted for a coherent line source were basically equivalent to that for a point source while incoherent line source showed considerable difference in frequency domain. P. Jean et al.[15] emphasized the importance of source type in the numerical modelling based on the calculation of 2.5-D BEM approach. They found the attenuation of conventional noise barriers for a coherent line source was much higher than that for an incoherent line source. Considering that the road/railway traffic noise is commonly assumed as one or more than one incoherent line sources[3, 12, 15, 16], using 2-D BEM modelling with coherent line sources must result in the overestimation of barrier performance. As a consequence, it was decided to carry out the calculations with a 2.5-D model using different numbers of incoherent point sources.

To validate a model nearly-enclosed barrier in three dimensions by BEM requires a certain amount of time for the high complexity of the computing process due to the complex geometry of the barrier. Based on the numerical method proposed in [14], a 2.5-D existing program was used to carry out 3-D boundary element calculations from solutions of problems defined in two-dimensional domains outside the associated cross-section. By using BEM to solve the acoustic problems in two-dimensional domains, the efficiency of the calculation is considerably improved. At the beginning of 2.5-D calculation, the source is assumed as coherent line source perpendicular to the page plane at first, which maintains the two-dimensional nature of the model. Subsequently by Fourier-like transformation the sound pressure fields created by

the coherent line source for the whole frequency spectrum will be converted into those radiated by a point source in three dimensions. The third position of the point source, defined relative to the plane where the two-dimensional calculation has been done, was considered in the existing program as well. Hence it was possible to calculate sound pressure for a line of such incoherent point sources.

The 2.5-D model of a nearly-enclosed barrier was obtained from the real prototype located on the viaduct of Metro 1 in Ningbo city, China, as shown in Figure 1. The noise barrier and the viaduct were assumed infinite uniform in construction along their length. In reality the barriers are installed on the viaducts so that there is no gap between the barriers and viaducts. However, on the basis of the BEM principle the distance between these two independent boundaries is at least larger than the element size[17]. Thus, this requires the geometry removal of the connections between them and therefore the boundaries of the viaduct and the barrier were integrated as a whole. These changes in the model are illustrated in Figure 2. The shape of vehicle source was simplified as a rectangle based on measurements of the stock Type B of China Railway Rolling Stock. The height assumed was 3.7 m and the width was 2.8m. It can be seen from Figure 2 that the source was placed at the outside wheel-rail interaction position. All the boundaries of the vehicle structure were made acoustically rigid. Taking into account reflections from the ground, the reflection from the image source symmetric to the source was also introduced into the model and the height of the viaduct above ground was 10 m.

To improve the precision requirement, the size of quadratic order element was defined as one tenth of the minimum wavelength. Furthermore,

(a) Inside the barrier (b) Outside the barrier

Figure 1: A prototype of the nearly-enclosed barrier located in Ningbo, China

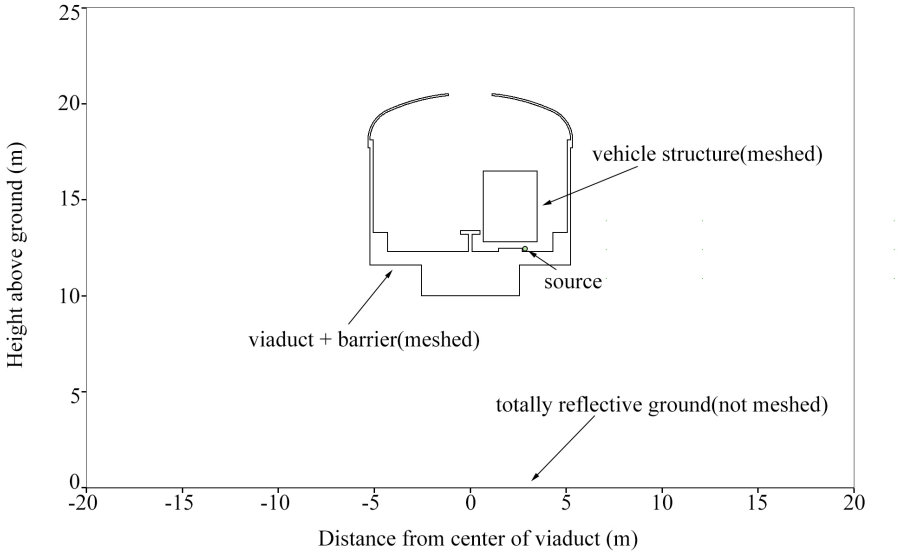

Figure 2: Numerical model for nearly-enclosed barriers on urban railway viaducts solved by 2.5-D BEM program

numerical predictions were calculated at third octave frequencies from 50 Hz to 1000 Hz.

A preliminary investigation was performed with the BEM predictions to understand the mechanism of the multiple reflections inside a nearly-enclosed barrier. In Figure 3, the blue areas represent pressure levels for the coherent line source as a function of frequency, fluctuating violently with a huge number of sharp-pointed peaks. Although the peak value decreases with increasing of frequency, with the rise in the number these peaks progressively dominate the sound pressure at a given receiver. Similar trends can be observed as well for the one-point source by the green areas, and these peaks retain their relative high levels at the similar frequencies. These peak levels would directly cause the deterioration of barrier performance that could not be ignored. According to the principle of resonance modes as referred in Section 1, several acoustic modes of the air cavity inside the barrier fully enclosed by Neumann boundaries, which corresponds the sound pressure level distribution at peak frequencies marked by red circles in Figure 3, are depicted. Figure 4&5 shows the 2D BEM results and the FEM acoustic modes. Good agreements on the contours and the peak frequency values are easily observable, which means these peak levels in the frequency domain were the

result of the resonance effect of the open-air cavity. Besides that, it is significant to note that the topped opening was not able to eliminate the resonance effect, but also leak high pressure levels into the surrounding region, thereby impacting seriously the noise reduction ability of the nearly-enclosed barrier. If some absorptive treatments are further added to the inner surface of the barrier, it is effective to improve the performance.

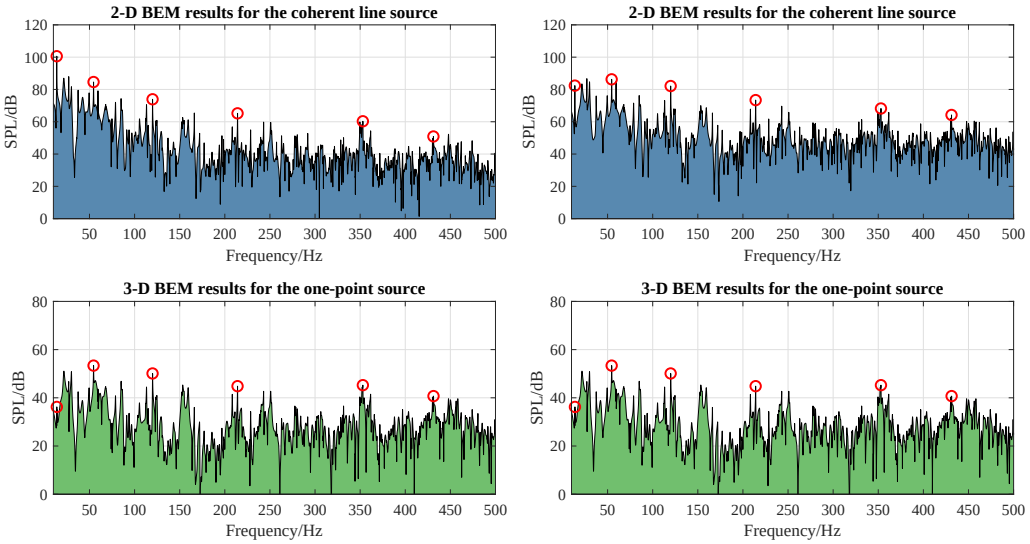

(a) 5 m away from the track central line (b) 40 m away from the track central line

Figure 3: The spectrum of sound pressure levels in the near and far field governed by the nearly-enclosed barrier(the receivers are positioned at the height of source)

3. Scale model measurement

To validate the predicted results for a nearly-enclosed barrier, the method of acoustic scale modelling was introduced. Scale model measurement has strict request to measurement environment. The test site has to be deliberately left as open as possible in order to emphasize the diffraction sound generated by the barrier model and prevent reflection sound caused by any reflecting surface close to the model from affecting the measured results. The site was finally selected as shown in Figure 6(a), which fully met the requirement specified previously. Considering the site limitations, the scale of the barrier model in our case was determined as 1:20.

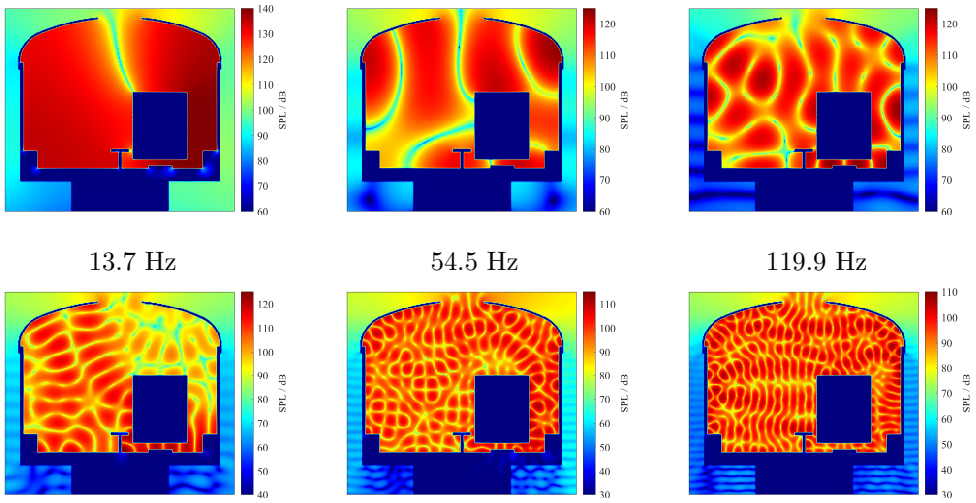

Figure 4: Pressure level distribution inside the barrier of 2-D BEM model

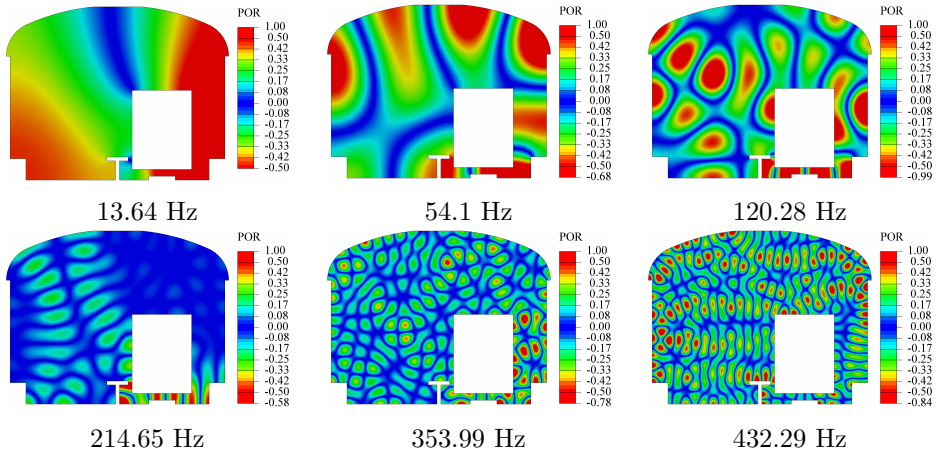

Figure 5: Several acoustic modes of the air cavity fully enclosed by the Neumann boundaries inside the 2.5-D BEM model of the nearly-enclosed barrier

3.1. Measurement apparatus

Generally loudspeakers and microphones are the indispensable transducers in an acoustic experiment. In order to send the electrical audio signal to the loudspeaker and receive it from the microphone synchronously, a collection of electronic apparatus was prepared. Miniature speakers with the size

of less than 1 mm^3 were chosen in our study since the space where the speaker located was less than 10 cm^3(approximately the size of an eraser). Commonly a normal-sized loudspeaker has a diameter of at least 30 mm, which is too large to be placed inside this model. The spectrum of the speaker was measured at several angles. It was found to be omni-directional when towards to the microphone. During the formal measurement for each test several employed loudspeakers emitted simultaneously white noise with one of the third octave spectrum from the signal output module. For these miniature loudspeakers the amplifiers and the power supply were selected accordingly. On the other hand, the highly sensitive B&K microphones 4189-A-021 satisfy the requirements of such high-precision, free-field measurement. They were powered from the supply offered by the DAQ signal output module. All the electronic apparatus were put under the model above ground, which did not appear in the transmitting path between the loudspeakers and the microphones affecting the measured results.

A VI project was designed in the LabVIEW development environment to transmit\receive electric signals. Figure 6(b) illustrates the signal flow graph of the measurement. It can be seen clearly that the original source signal was generated by the VI project from the laptop, transmitting to the output module, via the amplifier to the loudspeaker. In the meantime, sound pressure signal was received and preamplified by the microphone, via the input module back to the laptop, finally saved by the VI project. It is worth emphasizing that the VI project did not only play a role as a signal generator for activating the loudspeaker, it also undertook that of receiving, saving and analysing the signals from the receivers.

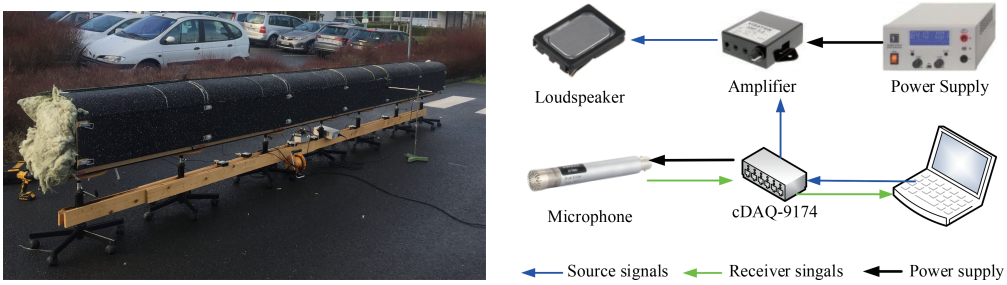

(a) Measurement site (b) Electronic apparatus

Figure 6: Scale measurement preparation

3.2. Scale model measurements

All barriers used in the experiment were a twentieth of the full scale numerical models. It was necessary to build simplified models for the complex structure so that sound diffraction towards the barrier would dominate attenuation measurements, facilitating comparison with the predictions from the BEM model which being 2.5-D in the space with infinitely long barriers. The tests were made in six configurations, of which the cross-sections were shown in Figure 7,

- Tests with viaducts and nearly-enclosed barriers(Figure 7(a1)(a2)).
- Tests with viaducts and double-straight barriers(Figure 7(b1)(b2)).
- Tests with viaducts(Figure 7(c1)(c2)).

The blue parts represent PC panels with a thickness of 5 mm and the brown parts are 9-mm-thick assembled wood planks. Tests were made with and without vehicle structures which were one twentieth the practicable 3.7x2.8 m^2 in full scale.

The 1:20 scale model was an assembly of six sections the length of each section being defined as 1 m since the metro vehicle is 19 m long and each train has six vehicles in reality. However, sound transmitting over the two ends of the model to the microphone must affect sound pressure level at the receivers. In order to reduce the end effect as much as possible, both barrier ends were filled with mineral wool to absorb sound(shown in Figure 6(a)).

There were twelve loudspeakers arrayed along the length of the six-section model. Each section of the model had two sources placed exactly at the position of each vehicle wheel in reality. The position in the cross section was close to the location of the wheel-rail interaction, in accord with that of the point source in the 2.5-D BEM model. A time-history signal of white noise was taken as the input of the sound source to the loudspeaker. Each of the signals was individually coherent but mutually incoherent to the others. Figure 8 and Table 1 present these co-ordinates and the numbers of the loudspeakers. The sampling position for the microphone was placed exactly at the cross-section where the 7th loudspeaker positioned.

Two sets of tests were taken to determine the third octave sound pressure levels outside the barriers. Tests were completed with the viaduct but without barriers(Figure 7(c1)(c2)) so that the attenuation could be calculated as the difference between the sound pressures measured in the presence and absence of barriers. Tests with viaducts and double-straight barriers(Figure

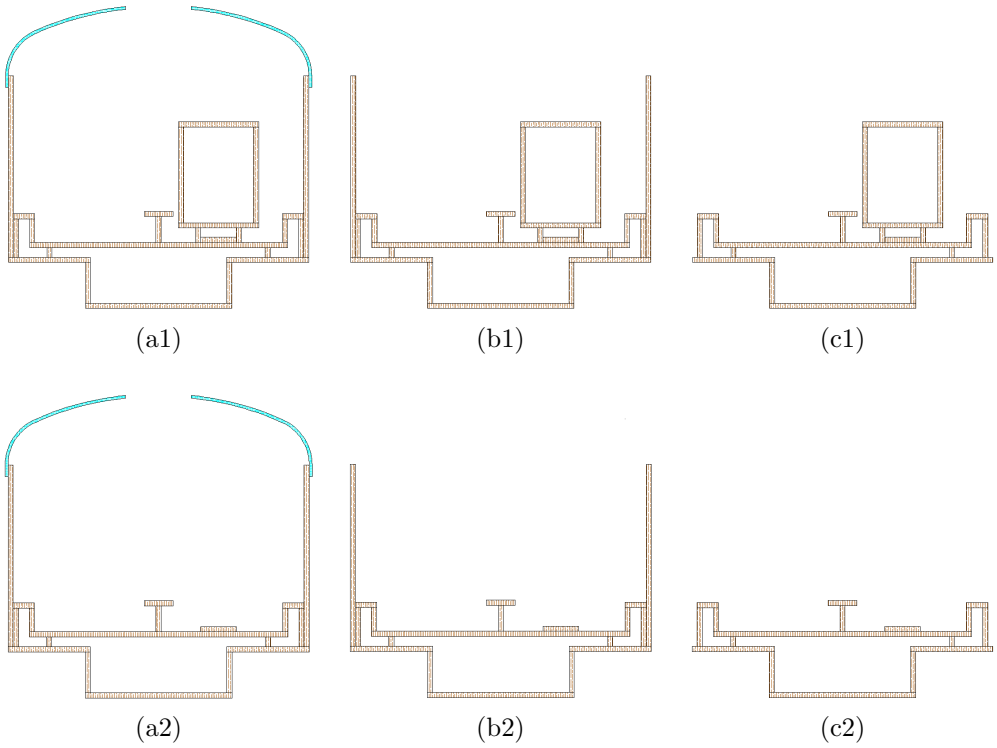

Figure 7: All the configurations of tested models. The upper row shows the models with vehicle structures and the lower row shows the models without vehicle structures.

7(b1)(b2)) were completed as well in order to understand the sound insulation property of the PC panels. In addition, the attenuations at the third octave band frequency from 1000 Hz to 20 kHz were tested to validate the 2.5-D BEM predictions from 50 Hz to 1000 Hz.

Table 1: Positions of loudspeakers and microphone in three co-ordinates(cm)

Loudspeaker			Microphone		
X_s	Y_s	Z_{si}(i=1,2,...,12)	X_r	Y_r	Z_r
3.6	0.5	-296.7, -233.7, -197.8, -134.8, -98.9, -35.9, 0, 63.0, 98.9, 161.9, 197.8, 260.8	25.6	19.0	0

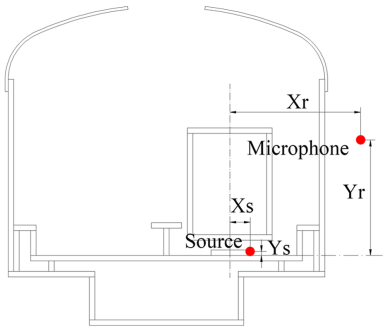

(a) Cross-section of the scale model

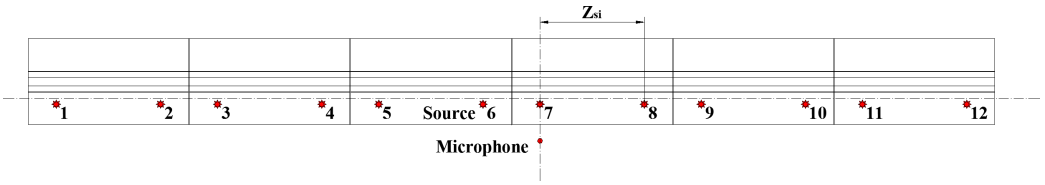

(b) Plan view of the scale model

Figure 8: Experimental arrangement for the nearly-enclosed scale barrier

3.3. Comparisons with BEM predictions

Predictions were carried out for the nearly-enclosed and double-straight barriers using the 2.5-D BEM program. The number of the incoherent point sources defined was one(the 7th) at first. Subsequently when numerical predictions were validated by measured results, the number would add up to four(the 5th, 6th, 7th and 8th) and finally to all twelve.

For one point source facing the microphone, Figure 9(a) shows plots of measured and predicted attenuations by the third octave band in the case of the double-straight barriers on the viaduct with and without vehicles. The predicted third octave source spectra was adjusted in the analysis so that the effective source spectra used in the BEM and scale models were identical (note that further frequencies in Section 3 will be given in the scale 1:20 for the sake of clarity). It is clear that as expected there is good agreement for each comparison between the measured results and those predicted by the 2.5-D BEM approach. The small deviation between the measured and predicted results is normal and permissible due to the non-idealised point source used for measurements.

Figure 9(b) shows the compared results for the nearly-enclosed barrier

on the viaduct. It is worth noting that the measured attenuations are much lower than those predictions regardless of the vehicle structures present, especially for high frequencies. And these measured results are as high as those measured for the double-straight type. With the finding of these significant differences between the measured and predicted results for the nearly-enclosed barrier, a strong argument can be made that the PC panels on the top were not considered to be acoustically rigid. This finding might be due to the sound insulation properties of the PC panels and wood planks which were not sufficiently high to reduce sound transmission through the nearly-enclosed barrier.

3.4. Sound insulation problem

The sound insulation propertas found abovey of material is usually evaluated by an acoustic physical term[18] i.e., sound transmission loss known as TL which is defined as 20 times the logarithm of the ratio of the acoustic pressure associated with the incident wave and that of the transmitted wave.

In terms of energy transfer, attenuation of the sound barrier(also known as Insertion Loss) depends precisely on the energy distribution of sound diffraction over the top, transmission through the barrier and reflection bounced off its surface. Considering the effect of ground absorption, the practical attenuation of the sound barrier is given as,

$$IL = A_d - C_t - C_r - C_G \tag{1}$$

where A_d denotes diffraction attenuation of the barrier top and side edges, which is the most important physical phenomenon in the noise reduction process. C_t is the correction value for sound transmission through the barrier, C_r is the correction for the sound reflection bounce off the barrier and C_G is the correction for ground absorption.

Typically, the diffraction attenuation A_d is much lower than the TL of high-density materials employed in the construction of the barrier, at least 10 dB. And in such case the correction for sound transmission C_t is negligible in the overall performance of the barrier. However, the predicted attenuations of the nearly-enclosed barrier have been found greatly higher than 20 dB over the frequency range of 1000 Hz-20 kHz shown in Figure 9(b). These values might be extremely close to those for the TLs of the employed materials so that the correction C_t could not be ignored in the calculation of the insertion loss. According to Eq (1) the measured attenuations were therefore lower

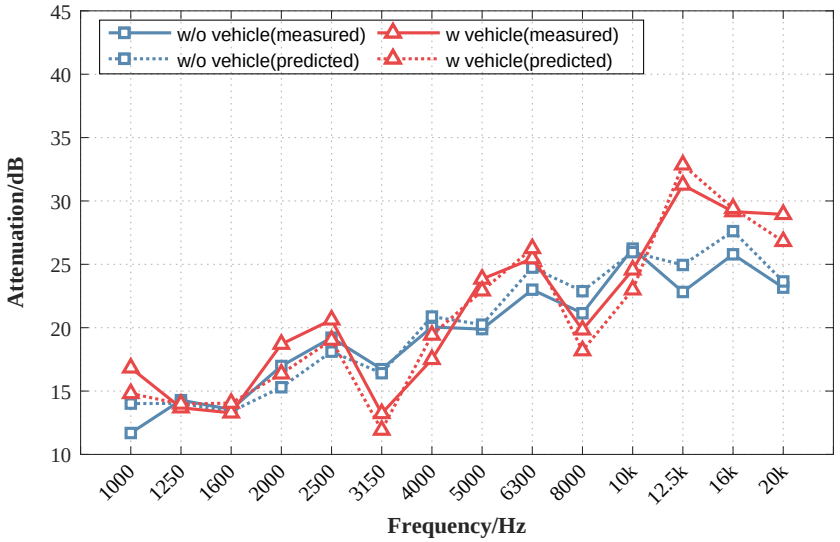

(a) Double-straight barrier on the viaduct

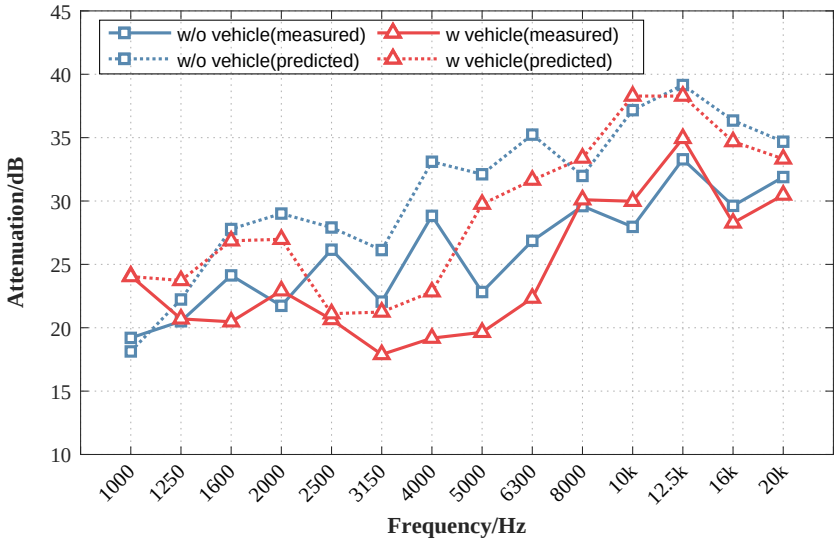

(b) Nearly-enclosed barrier on the viaduct

Figure 9: Measured and predicted attenuations for the model(a) double-straight barrier(Figure 7(b1)(b2)); (b) nearly-enclosed barrier(Figure 7(a1)(a2))

than our expectations.

Since the barrier attenuation is frequency dependent and so is the impact

of transmission loss, to better understand their relationship, the comparisons for high frequencies between the predicted attenuations for the nearly-enclosed and the double-straight barrier and the measured TLs for the PC panels are illustrated in Figure 10. The blue and red curves without symbols represent the TLs for PC panels measured by Woo-Mi Lee et al.[19] with a thickness of 4 mm and 8 mm, respectively. On account of the thickness of the PC panel in our test being 5 mm, its TL curve must be sensibly lying in the region between these two curves. At the frequency higher than 4000 Hz, the value of TL theoretically tends to increase 6 dB per octave band. As a consequence, the approximated transmission loss of the employed PC panels in our test was estimated reasonably for each third-octave band of interest according to the discussion above, which is represented by the green dotted line shown in Figure 10. The blue and red curves with rectangular symbols in Figure 10 represent the predicted attenuations for the nearly-enclosed and double-straight barrier, respectively. It is obvious that at frequencies from 1000 Hz to 2000 Hz and from 4000 Hz to 12.5 kHz the approximated TLs are quite close to the predicted attenuations for the nearly-enclosed type, but much higher than those for the double-straight type by at least 10 dB. Hence the correction term of sound transmission must be taken into account and in such case the boundary condition of two arched PC panels cannot be considered as totally reflected in the BEM model for the nearly-enclosed barrier. Therefore, we can conclude that the insufficient insulation property of the PC panels must be the foremost reason for the considerable differences between the predicted and measured results mentioned previously for the nearly-enclosed barrier.

To improve the sound insulation property of the arched parts for the nearly-enclosed barrier so that better measured attenuations could be tested, a kind of material that provides good sound insulation as well as flexibility was needed. The transmission loss of a typical single-layer material is theoretically divided into three distinct performance regions developed from the frequency range: I. stiffness and resonance region, II. mass region and III. coincidence region. Region I typically ranges below 200 Hz[20] where the TL is controlled by the stiffness and the resonance frequency of the material. In Region II the relationship between TL and frequency is mainly controlled by the mass of material, which is known as the mass law: each time the mass is doubled the TL increases 6 dB. This law continues to meet the critical frequency f_c at which sound waves incidents are able to efficiently transfer energy to the panel. This phenomenon is called the "coincident effect" which

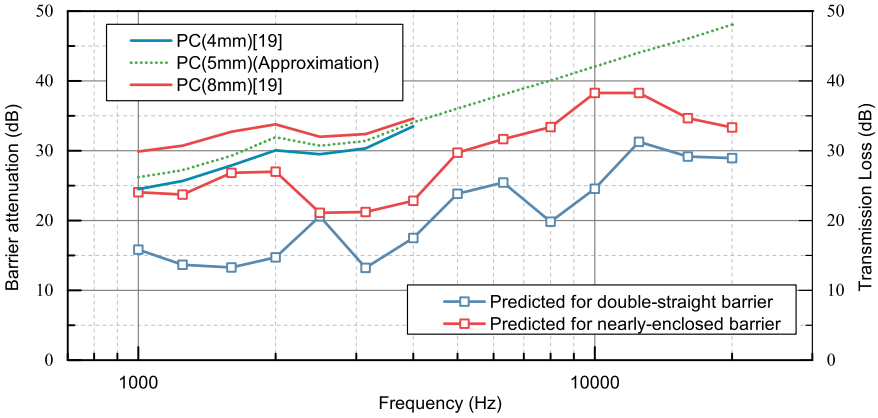

Figure 10: Comparison between the predicted attenuations of barriers and the TLs of PC panels

severely influences the sound insulation performance of the material. The critical frequency for a single-layer isotropic homogenous material is defined as,

$$f_c = \frac{c^2}{2\pi t}\sqrt{\frac{12\rho_m\left(1-\sigma^2\right)}{E}} \tag{2}$$

where c denotes sound speed, t is the thickness of material and ρ_m is mass of the panel per unit surface area. E and σ are Young's modulus and Poisson's ratio of the material, respectively.

Taking for instance the 5-mm-thick PC panel with an average density of 1.2 g/cm^3 employed in the scale measurement, the TL fluctuates violently in Region I, then increases by 6 dB per octave in Region II and suddenly declines significantly when approaching critical frequency. At higher frequencies the TL continues to increase by 6 dB per octave again in Region III. The critical frequency for the PC panel equals approximately 3200 Hz calculated by Eq. 2. The value of critical frequency is in the range of interest, which means the employed PC panels in the scale measurement showed their sound insulation performance not only in Region II but also in Region III. Recall from Figure 10 that in Region II below 3200 Hz the differences between the TLs and the predicted attenuations for the nearly-enclosed model were less than 10 dB, and in Region III the loss of TL caused by the coincident effect leads the TL much closer to the increased attenuation with increasing frequency. Once more, the further analysis based on the sound insulation theory proves that the PC panels employed in our test were not able to sufficiently insulate the

traffic noise.

From these findings we can summarize that the material with high density has a good sound insulation property due to the mass law. On the other hand, with high critical frequency the material shows its TL performance in the test almost in Region II to avoid the coincident effect. Hence it is better to select a kind of transparent material with high density, high critical frequency and high flexibility for the arched shape. According to this description, the 10-millimetre-thick rubber was chosen. The TL of the arched parts must be improved considerably by the heavy mass owing to the high thickness of rubber. Although the density can be expected to be between 0.96 g/cm^3 and 1.3 g/cm^3f only as large as that for the PC panels, with a low Young's Modulus(0.001-0.0022 GPa) its critical frequency can be up to over 40 kHz so that its TL performs only by the mass law in the scale model measurement. Furthermore, it is quite easy to reshape. Thus, it was possible to reduce the differences between measured and predicted results by the rubber covering with no need to worry about the transparency of the material.

For the sake of comparison between the scale model with and without rubber, the rubber was only applied to coat the whole model of barrier, not to act as the alternative to any existing materials constructing the barrier. Figure 6(a) shows its application in our scale model measurement.

3.5. Effect of rubber covering

In order to improve the sound insulation, repeated scale tests with additional 10-mm-thick rubber covering on the outer surface of the model were carried out. Figure 11 illustrates all the configurations of the tested models with the rubber covering. The black parts represent the rubber coating on all the outer surfaces of the barrier. In addition, to test the effect to the nearly-enclosed barrier(Figure 11(d1)(d2)), a comparison for the double-straight barrier between the model with and without the rubber covering was made as well. Figure 12 compares the measured results with the corresponding BEM predictions for the double-straight model and the nearly-enclosed barrier, respectively. Identically to the previous observations, the measured results for the double-straight barrier with the rubber covering correspond to the 2.5-D BEM predictions, and the differences between the measured results and the predictions are a little smaller than those for the case without the rubber covering(Figure 9(a)). This proves the employed wood planks were sufficiently thick to insulate sound when the barrier shape was straight. And with the help of the rubber covering the improvement was negligible. Then

to compare with the nearly-enclosed barrier it is encouraging that with the addition of the rubber covering the agreement between the measured and predicted results was obviously improved comparing with that shown in Figure 9(b) . This agreement provides very strong evidence that the employed PC panels cannot be assumed to be totally reflective panels to preventing sound from transmitting through when the barrier has a nearly-enclosed shape, and adding a cover of material with good sound insulation to the surface of the PC panels is a practicable way to improve the barrier attenuation, to bring it close to the expectation of 2.5-D BEM model.

As a result, it can be concluded that generally there is good agreement between the measured results obtained in the scale model with the rubber covering and those predicted by the 2.5-D BEM model of the nearly-enclosed barrier.

On the basis of the agreement between the measured results and predic-

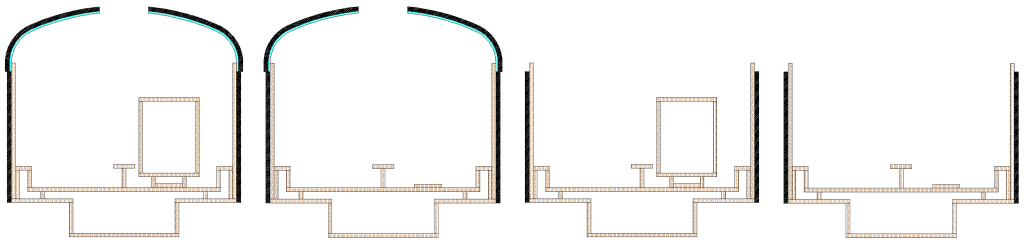

Figure 11: The configurations of the tested models with the rubber covering

tions for the nearly-enclosed barrier, the number effect of incoherent point sources on the barrier attenuation was analyzed. In order to validate the 2.5-D BEM predictions with several incoherent point sources the number of loudspeakers was changed as mentioned previously. Figure 13 provides the information about the results for different numbers of incoherent point sources for the nearly-enclosed barrier. Before the discussion on the number effect of incoherent point sources, it is necessary as a starting point to verify the predictions by the measured results. Apparently each comparison shows good agreement, as our expectation. Then, we found that the curves in Figure 13 vary widely with increased frequency: some are extremely fluctuating, while others tend to smooth.

In Figure 13, it is easy to understand the growth of attenuation fluctuates seriously with frequency for one point source(blue curves). And yet it is

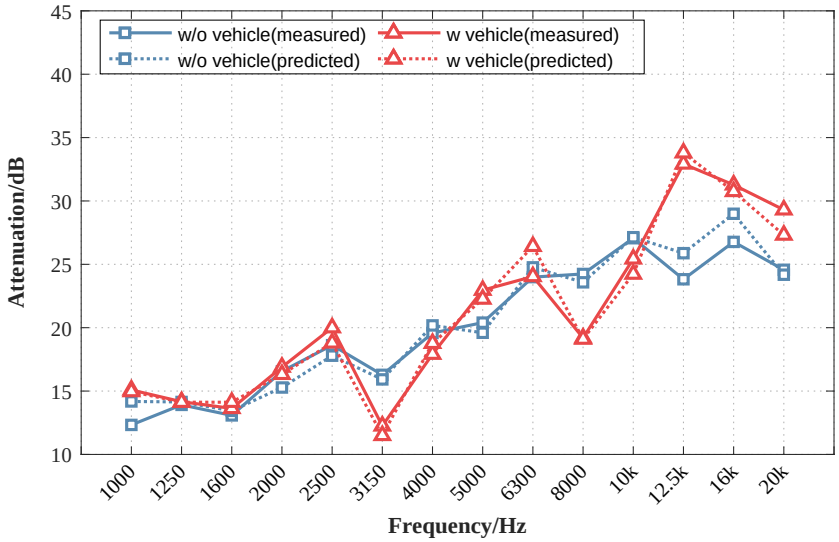

(a) Double-straight barrier on the viaduct

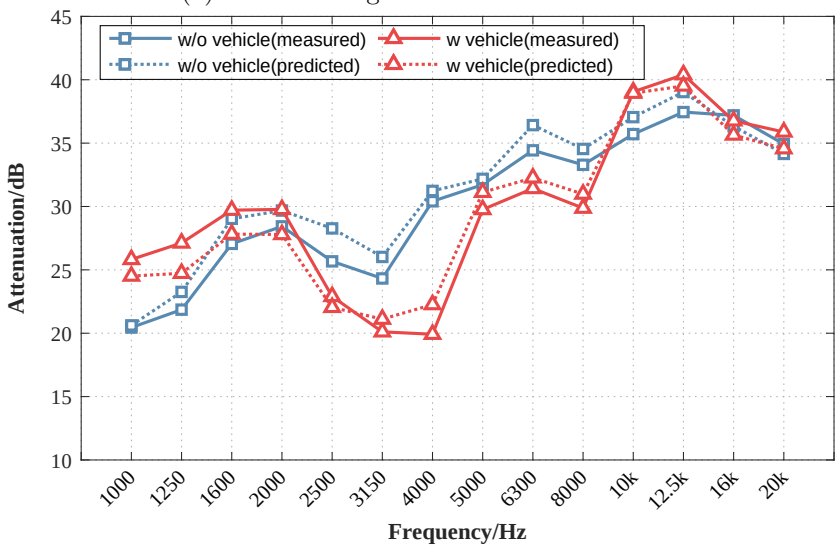

(b) Nearly-enclosed barrier on the viaduct

Figure 12: Measured and predicted attenuations for the model with the rubber covering(a) double-straight barrier(Figure 11(e1)(e2)); (b) nearly-enclosed barrier(Figure 11(d1)(d2))

interesting that the attenuation tends to increase smoothly as the number of incoherent point sources increases to four(red curves). When increased to the maximum number of sources(green curves), the attenuations have a visible decline at each frequency band in comparison with those of four-point source.

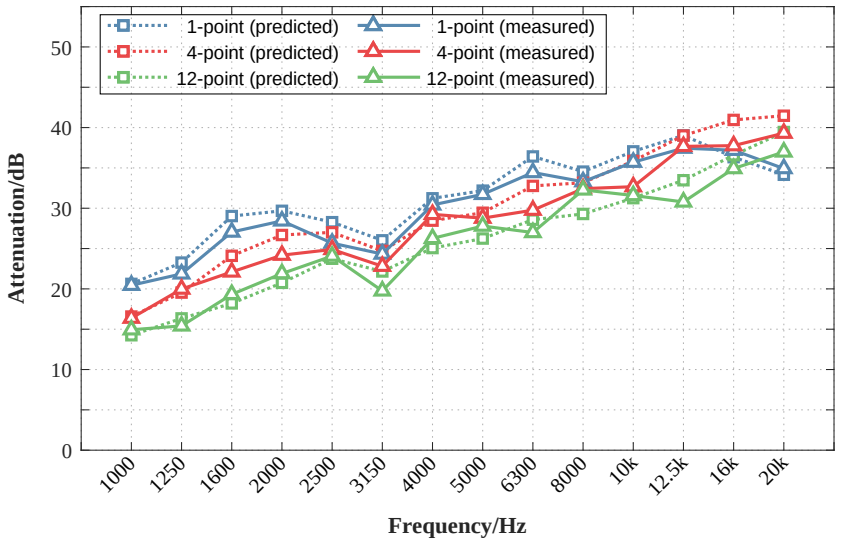

(a) Without vehicle

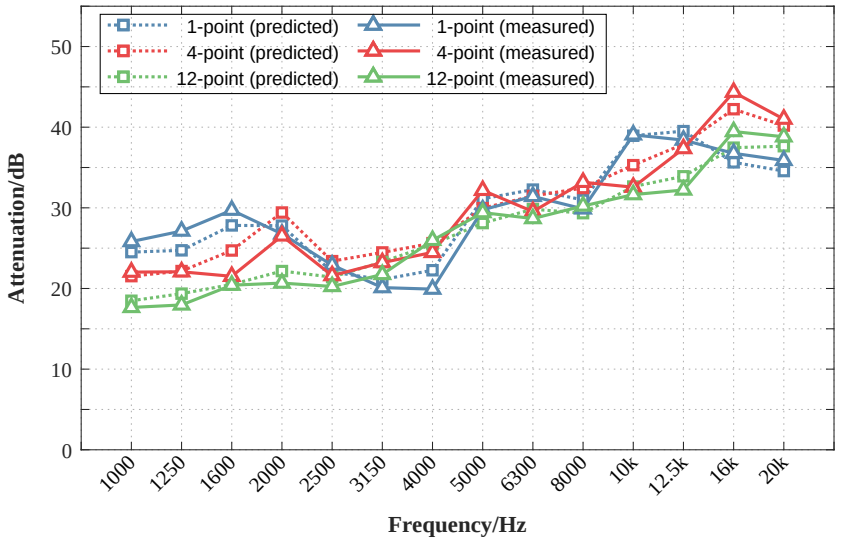

(b) With vehicle

Figure 13: Measured and predicted attenuation for the nearly-enclosed barrier: (a) without vehicle(Figure 11(d2)); (b) with vehicle(Figure 11(d1))

In addition, the comparison of the results between the model with and without the vehicle structures was also considered. The frequency-attenuation curves with the vehicle structures(Figure 13(b)) fluctuate much more than

those without the vehicles(Figure 13(a)), even for the smoothest curves corresponding to the twelve incoherent point sources. This is due to the multiple reflection between the vehicle structure and the inner surface of the barrier, which can be reduced by treating the inner surface with an absorbent material.

All the findings in the scale measurement for the nearly-enclosed model with a rubber covering demonstrate good agreement with those predicted by the 2.5-D BEM approach for each the third octave band from 1000 Hz to 20 kHz. To summarize, it can be assumed that the acoustic performance of the nearly-enclosed barrier investigated by the 2.5-D BEM predictions for incoherent point sources are reliable.

4. 2.5-D BEM predictions

The 2.5-D BEM program was used to make predictions of attenuations reduced by the nearly-enclosed barrier in order to identify its acoustic performance in the surroundings. Run times with the complex geometry of the nearly-enclosed barrier and railway vehicle simulation were excessive. In order to reduce calculation times only the model with viaducts and nearly-enclosed barriers but without rubber coverings(Figure 7(a1)) was calculated for the whole frequency spectrum. Identically to the measurement, the calculation was also completed without barriers(Figure 7(c1)) for attenuation analysis.

4.1. Rearrangement of source and receiver positions

As we discussed in a previous article[21], based on the diffraction theory the receiver positions need to be in all six significant acoustic areas: bright zone, transition zone and shadow zone in the near field and far field, respectively. The bright zone and transition zone for the nearly-enclosed barrier were elongated and quite close to the source on the horizontal axis due to the special shape of its top. The rest is therefore the shadow zone covering most of the acoustic field. Considering that it is impossible to develop any construction projects at the two former zones, our observation in this section is focused on the performance at the shadow zone. Within this zone the receiver positions were in the near field and far field separately. For the frequency range of interest(50 Hz- 1000 Hz in the full scale) the boundary between the near field and far field is located at around 14 meters away from the source. Notice that further frequencies in Section 4 will be given

in the full scale. Consequently, by the grid-form method referred to in [21], predictions were made at receivers placed at the four receiver distances(5, 10, 20 and 40 m from the centre of the track) on the horizontal axis and at the three receiver heights(1.5 m above, 1.5 m below and at the height of the track) on the vertical axis. Figure 14 illustrates these receiver positions. Given the large number of receiver positions, it was important to assign a name to each receiver. The name of each receiver begins with "M". The first number represents the column number which is smaller as the receiver gets closer to the source, whereas the second number represents the row number which is larger as the receiver gets closer to the ground. A symbol like "M1-" "M -1" which will be seen in later sections represents, for example, all the receivers in the first column or the first row, respectively.

Unlike only one point source simulated on the cross-section of the scale

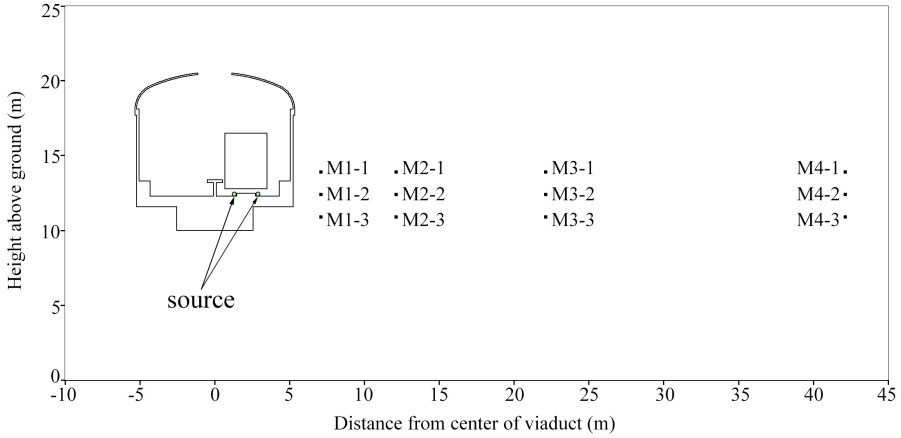

Figure 14: Source and receiver positions in the 2.5-D BEM calculation

model in the measurement, the noise sources were modelled as two incoherent point sources on the cross-section positioned at the approximate height of two rail-wheel interaction positions(represented by two dots in Figure 14). Note that the source to receiver distance discussed below represents the distance horizontally away from centre of track(also the centre of two incoherent point sources on the cross-section). Identically to the previous calculation, the predictions for different numbers of sources(1, 4 and 12 incoherent point sources arrayed along the length of barrier) were made as well for all the receivers mentioned above. Each distance perpendicular to the page between the source and receiver is also the same as that in the previous calculations.

In the 2.5-D calculations, sound pressure was predicted for several individual frequencies with a linear spacing of 0.1 Hz per third octave band ranging from 50 Hz to 1000 Hz. The energy for all the incoherent point sources in the model was summed within each band yielding the third octave band spectrum. Eventually the attenuation spectrum was calculated by the logarithmic ratio of the energy obtained between the model without and with the barrier.

4.2. Near field

Figure 15&16 show the predicted attenuations for the receivers in the near field for different numbers of incoherent point sources. For the source to receiver distance of 5 m there is a consistent pattern in the results obtained, with the attenuation varying with the third-octave band for a given number of sources, but to different degrees as observed in Figure 15. Among them receiver M1-1 is the most greatly affected by changes in the band for a given number of sources while there is the least effect for M1-3. And it can be seen more obviously that the attenuation obtained with the highest receiver M1-1 is significantly greater than that obtained with the lowest receiver M1-3 for all the third-octave bands of interest. That means the attenuation increases with the increased height of receivers for all the cases examined in M1- and the effect is very considerable.

However, with the increased number of sources, attenuation always decreases for a given receiver, and more importantly, it tends to fluctuate less. Taking an example for receiver M1-1, the global maximum of attenuation for one-point source is 41.61 dB at 630 Hz, while there are two local maximums, 31.94 dB and 28.56 dB at 250 Hz and 100 Hz, respectively. For the four-point source the increase of attenuation from 630 Hz, to 1000 Hz is positive but slow so that the global maximum is located at the maximum band of interest, i.e. 41.83 dB at 1000 Hz. And obviously there is only one local maximum: 27.89 dB at 100 Hz. For the twelve-point source the attenuation increases smoothly with the increased band and therefore it is difficult to find a local maximum. Again, the global maximum is located at the maximum band of interest, i.e. 39.34 dB at 1000 Hz.

The attenuation for the source to receiver distance of 5 meters in general is higher than 13 dB for each band, and from 400 Hz to 1000 Hz it is even higher than 20 dB. While for the source to receiver distance of 10 m the attenuation is on average higher than 10 dB, and from 400 Hz to 1000 Hz it is even higher than 15 dB. Figure 16 shows the attenuation achieved for the

source to barrier distance of 10 m for all configurations examined. Again, it can be observed that there is a similar pattern in the results obtained with the attenuation varying with the third-octave band for a given number of source. However, unlike the predictions for receiver in M1- the attenuations for the receiver in M2- are not greatly affected by changes in the height of the receiver for a given third-octave band ranging from 50 Hz to 400 Hz, although there is a small effect on attenuation from 500 Hz to 1000 Hz.

For the source to receiver distance of 10 m with the increased number of source attenuation decreases again and tends to fluctuate less for a give receiver. There is a similar trend for each receiver in M2- that the attenuation ranging from 400 Hz to 1000 Hz firstly increases and then decreases for one-point source, then increases slowly when the number increases to four, and finally increases linearly for the twelve-point source. Because of this, the associated frequency of the global maximum increases with the increased number of sources, i.e. the global maximum for M2-1 is 25.33 dB, 28.13 dB and 27.2 dB at 630 Hz, 800 Hz and 1000 Hz for the one-point, four-point and twelve-point source respectively. On the other hand the global minimum of attenuation for the one-point source for the receiver in M2- can be seen clearly at 160 Hz with the value of approximately 6 dB, and it is the most distinct trough in Figure 16. Nevertheless, this trough gradually disappears for the four-point and twelve-point sources.

The following general conclusions can be drawn from the above: first, the attenuation with an average of approximately 15 dB can be achieved in the near field; secondly, the height effect of the receiver on attenuation is significant for the source to receiver distance of 5 m while that for the source-receiver distance of 10 m is almost invisible; thirdly, the increased number of source can result in the smoother and lower attenuation.

4.3. Far field

Figure 17 &18 show the predicted attenuations for the receivers in the far field for different numbers of incoherent point sources. For the source to receiver distance of 20 m there is again a similar trend in the results obtained, with the attenuation varying with the third-octave band for the whole frequency range for a given number of sources(as observed in Figure 17). However, an opposite trend for the height effect of receivers can be observed in M3- that attenuation decreases with the increased height of receivers for a given number of sources but the effect is very small.

With the increased number of sources, attenuation decreases for a given receiver. A similar noticeable trough can be observed at 160 Hz in Figure 17 for one-point source, but it is surprising that it is a negative value and its magnitude increases with decreased height for the receiver in M3- with the lowest value of -2.46 dB. However, for all cases of the other two source types the magnitudes of attenuations are always positive since the attenuation is more stable with smaller fluctuations. For a given receiver there is also a peak at 250 Hz for the one-point source but less obviously for the four-point source, and it finally disappears for the twelve-point source. The attenuation for the twelve-point source for the receiver in M3- fluctuates within a small range of 6-13 dB ranging from 50 Hz to 400 Hz, and it increases slowly from 400 Hz to 1000 Hz.

The attenuation for the source to receiver distance of 20 m average is lower than 20 dB for each band, while for the source to receiver distance of 40 m the attenuation is on average lower than 10 dB. Figure 18 shows the attenuation achieved for the source to barrier distance of 40 m for all configurations examined. Again, it can be observed that there is a similar pattern in the results obtained, with the attenuation varying with the third-octave band for a given number of sources. And similar to those in Figure 17 attenuation decreases with the increased height of the receiver for a given number of sources, but the effect is quite small.

Unlike the negative value of global minimum for all the receivers in M3- for the one-point source, there is a negative attenuation as the global minimum only at 160 Hz for M4-2 for the one-point and the four-point source. Apart from that, for the source to receiver distance of 40 m with increased number of sources, attenuation for the receiver in M4- decreases and fluctuates less again for a give receiver. For the global maximum, the associated frequency is unchanged with the value of 50 Hz. And the magnitude firstly increases and then decreases with increasing number of sources, i.e. for M4-1 it is 17.80 dB, 18.58 dB and 16.10 dB for the one-point, four-point and twelve-point source, respectively.

The following general conclusions can be drawn from the above: first, the attenuation with an average of approximately 10 dB can be achieved in the far field; secondly, the performance in the far field reduces with increasing height of receivers but the effect is very small, in other words, the performance is relatively unaffected by the height of receivers; thirdly, the increased number of sources can result in the attenuation being much smoother and lower, especially eliminating the negative value induced by the small number

of sources.

5. Discussion and conclusions

The 2.5-D BEM program developed for incoherent point source calculations was used to solve the practical problem of assessing the acoustic performance outside a nearly-enclosed barrier with infinite length. The results of a preliminary investigation calculated by the 2.5-D BEM program showed that there were amounts of peaks in the frequency domain of sound pressure in the surroundings of the nearly-enclosed barrier. With good agreement between the sound pressure distributions at the peak frequencies and the corresponding acoustic modes of the air cavity inside the barrier, a reasonable explanation of these peaks was given that when the shape of the barrier was nearly-enclosed, the acoustic resonance effect generated by the open air cavity could result in extremely high levels at the resonance frequencies, directly deteriorating the barrier performance. To suppress the resonance effect the additional absorptive treatments on the inner surface of the barrier is proposed for further research.

To validate the predictions a series of scale model measurements were made since the scale modelling technique allowed the effect of the employed material on the barrier performance to be more realistic. It was shown from the comparison that there was a significant deviation between the measured and predicted results for the nearly-enclosed barrier, but good agreement for the double-straight barrier. Measured attenuations for the nearly-enclosed barrier were obviously higher than those for the double-straight type in the mid-frequency range, while at high frequencies, attenuations for the nearly-enclosed barrier were almost the same as those for the double-straight type. More importantly, the measured results for the nearly-enclosed barrier were much lower than those predicted by the BEM, which may result from the insufficient sound insulation of the PC panels.

Based on the sound insulation theory and the measured TLs in [19], the transmission loss of the 5-mm-thick PC panels employed in the scale model was estimated. The comparisons show that the predicted attenuations for the nearly-enclosed type were quite close to the transmission loss of the PC panels in the frequency range of interest. According to the calculation of barrier attenuation in the form of energy transfer, the correction for sound transmission could not be ignored. Therefore, the insufficient sound insulation of the PC panels was identified to be the main cause of the differences

between the measured and predicted attenuations for the nearly-enclosed barrier. As mentioned above, the PC panels, employed for the arched parts in the full-scale prototype of the nearly-enclosed barrier in China, have a thickness of only 6.5 mm, a little thicker than those employed in the scale model in our test. Thus, the sound insulation of the PC panels in the actual project are considered to be not sufficient as well. The need for transparent material with better sound insulation and high flexibility was long ignored and urgent for the arched parts, both in the scale model tests and the actual projects.

With the help of 10-mm-thick rubber, a supplementary measurement was developed for solving the difficulty. Fortunately, the predictions of one-third octave band levels using the 2.5-D BEM program were shown to be comparable with the 1:20 scale measurements by fully coating all surfaces with rubber so that confidence can be given in the BEM predictions for the whole field. The compared results also reconfirmed the insulation problem of the PC panels for the nearly-enclosed barrier. In addition, the predictions for the four-point and twelve-point sources were shown to be comparable with the measured results, which provides us the opportunity to discuss the number effect of incoherent point sources.

Considering the complex sound field distribution caused by the specific structure of a nearly-enclosed barrier, in order to understand thoroughly the barrier performance, the receiver positions were rearranged according to [21]. The rearrangement approach based on the diffraction theory was used to estimate the performance of the sound barrier in each area with different acoustic features.

As expected, the attenuation of the nearly-enclosed barrier averaged around 15 dB in the near field and around 10 dB in the far field. This indicates that the nearly-enclosed type has a more effective and efficient performance on the premise that all the boundaries are acoustically rigid. This kind of barrier with high attenuation designed by the modification of shape requires the employed material with sufficiently high sound insulation property. Otherwise the design will be largely failed and not economical for the practical use.

It was also shown that the attenuation decreased with increasing source-receiver distance, while it increased with increasing height of receivers only in the column which was the closest to the source in our study. For the other three source-receiver distances the height effect of receiver was almost negligible. The number effect of incoherent point sources was also taken into account for modelling railway traffic noise. Apparently, the increased num-

ber of source can result in much smoother and lower attenuations for all the areas, especially eliminating the negative value induced by the small number of sources. In addition, the resonance effect referred to previously can be the reasonable explanation of the negative values of the attenuations in the far field.

[1] A. Jolibois, J. Defrance, H. Koreneff, P. Jean, D. Duhamel, V. Sparrow, In situ measurement of the acoustic performance of a full scale tramway low height noise barrier prototype, Applied Acoustics 94 (2015) 57–68 (2015). doi:10.1016/j.apacoust.2015.02.006.
URL http://dx.doi.org/10.1016/j.apacoust.2015.02.006

[2] X. LI, D. Yang, W. GAO, Y. LUO, Study on Vibration and Noise Reduction of Semi- or Fully- Enclosed Noise Barriers of High Speed Railways, Noise and vibration control 38 (Z1) (2018). doi:10.3969/j.issn.1006-1355.2018.Z1.002.

[3] G. R. Watts, D. C. Hothersall, K. V. Horoshenkov, Measured and predicted acoustic performance of vertically louvred noise barriers, Applied Acoustics 62 (11) (2001) 1287–1311 (2001). doi:10.1016/S0003-682X(00)00101-8.

[4] G. R. Watts, Acoustic performance of parallel traffic noise barriers, Applied Acoustics (1996). doi:10.1016/0003-682X(95)00031-4.

[5] D. J. Oldham, C. A. Egan, A parametric investigation of the performance of multiple edge highway noise barriers and proposals for design guidance, Applied Acoustics (2015). doi:10.1016/j.apacoust.2015.03.012.

[6] C. Yang, J. Pan, L. Cheng, A mechanism study of sound wave-trapping barriers 134 (3) (2013). doi:10.1121/1.4816542.

[7] W. Bowlby, L. F. Cohn, A model for insertion loss degradation for parallel highway noise barriers, The Journal of the Acoustical Society of America 80 (3) (2005) 855–868 (2005). doi:10.1121/1.393909.

[8] M. R. Monazzam, S. M. B. Fard, Impacts of Different Median Barrier Shapes on a Roadside Environmental Noise Screen, Environmental Engineering Science (2011). doi:10.1089/ees.2010.0269.

[9] G. R. Watts, N. S. Godfrey, Effects on roadside noise levels of sound absorptive materials in noise barriers, Applied Acoustics (1999). doi:10.1016/S0003-682X(99)00007-9.

[10] S. Kirkup, The BEM in Acoustics (1998) 161 (1998).

[11] A. Muradali, K. Fyfe, A study of 2D and 3D barrier insertion loss using improved diffraction-based methods, Applied Acoustics 53 (1-3) (2002) 49–75 (2002). doi:10.1016/s0003-682x(97)00040-6.

[12] P. Jean, A variational approach for the study of outdoor sound propagation and application to railway noise, Journal of Sound and Vibration (1998). doi:10.1006/jsvi.1997.1407.

[13] R. Seznec, Diffraction of sound around barriers: Use of the boundary elements technique, Topics in Catalysis (1980). doi:10.1016/0022-460X(80)90689-6.

[14] D. Duhamel, Efficient calculation of the three-dimensional sound pressure field around a noise barrier, Journal of Sound and Vibration 197 (5) (1996) 547–571 (1996). doi:10.1006/jsvi.1996.0548.

[15] P. Jean, J. Defrance, Y. Gabillet, The importance of source type on the assessment of noise barriers, Journal of Sound and Vibration 226 (2) (1999) 201–216 (1999). doi:10.1006/jsvi.1999.2273.

[16] R. Makarewicz, J. Jarz, A. Preis, Rail Transportation Noise With and Without a Barrier, Applied Acoustics 26 (July 1988) (1989) 135–147 (1989).

[17] R. Bialecki, R. Dallner, G. Kunhn, Minimum distance calculation between a source point and a boundary element, Engineering Analysis with Boundary Elements 12 (1993) (1994) 211–218 (1994).

[18] J. Zhao, X. M. Wang, J. M. Chang, Y. Yao, Q. Cui, Sound insulation property of wood-waste tire rubber composite, Composites Science and Technology (2010). doi:10.1016/j.compscitech.2010.03.015.

[19] J. H. Lee, J.-R. Park, W.-M. Lee, J.-H. Son, I.-H. Kim, K. S. Kim, Sound Insulation Properties of Polymer Soundproof Panels, Journal of Korean Society of Environmental Engineers (2014). doi:10.4491/ksee.2013.35.8.592.

[20] Y. Yang, B. Li, Z. Chen, N. Sui, Z. Chen, M. U. Saeed, Y. Li, R. Fu, C. Wu, Y. Jing, Acoustic properties of glass fiber assembly-filled honeycomb sandwich panels, Composites Part B: Engineering (2016). doi:10.1016/j.compositesb.2016.04.046.

[21] Q. Li, D. Denis, Y. Luo, H. Yin, Improved Methods for In-situ Measurement Railway Noise Barrier Insertion Loss, Transactions of Nanjing University of Aeronautics and Astronautics (2018).

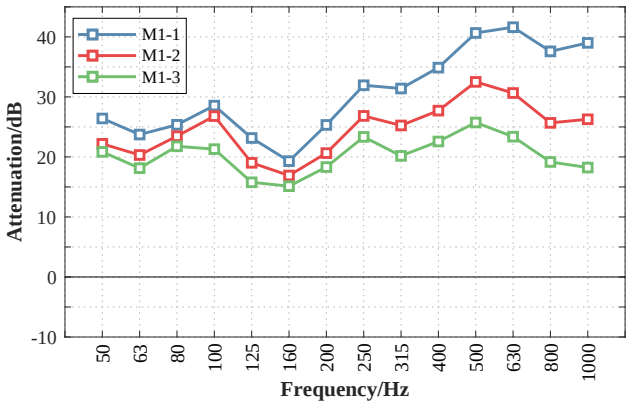

(a) one-point source

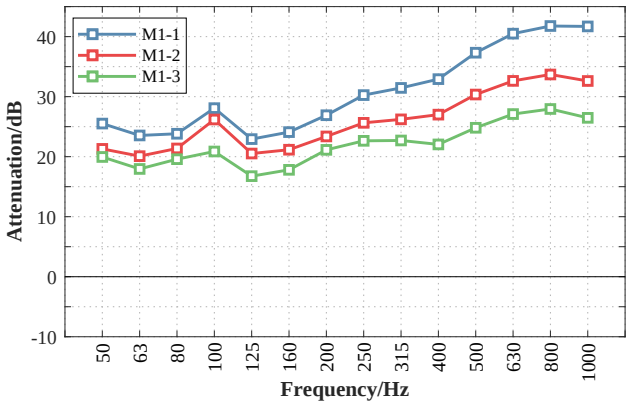

(b) four-point source

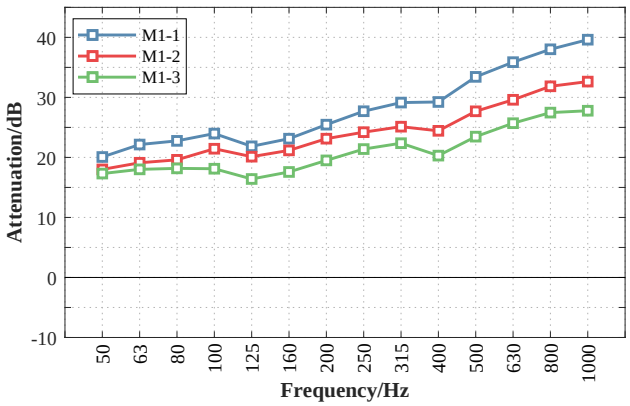

(c) twelve-point source

Figure 15: Predicted attenuations for the source to receiver distance of 5 meters

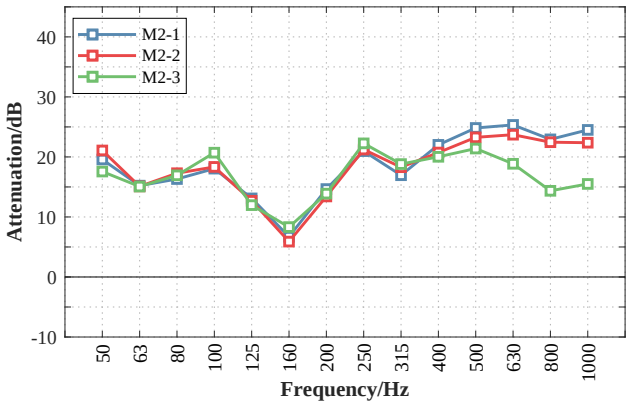

(a) one-point source

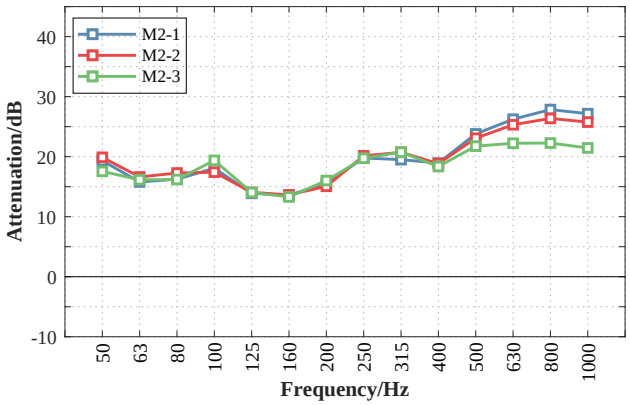

(b) four-point source

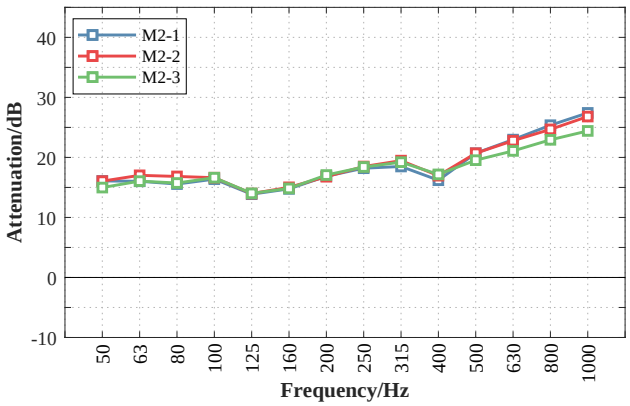

(c) twelve-point source

Figure 16: Predicted attenuations for the source to receiver distance of 10 meters

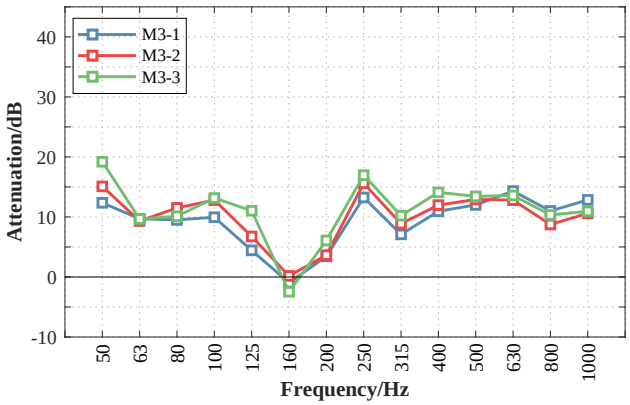

(a) one-point source

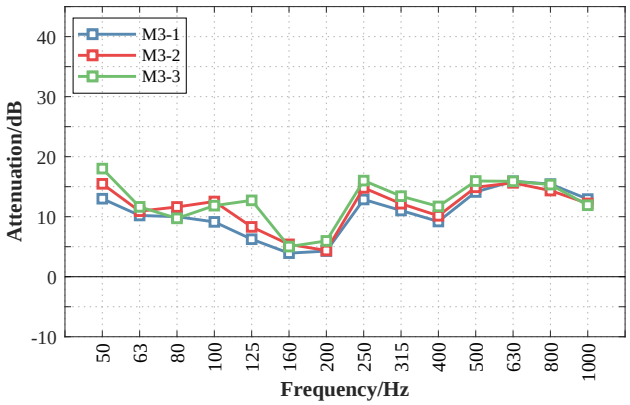

(b) four-point source

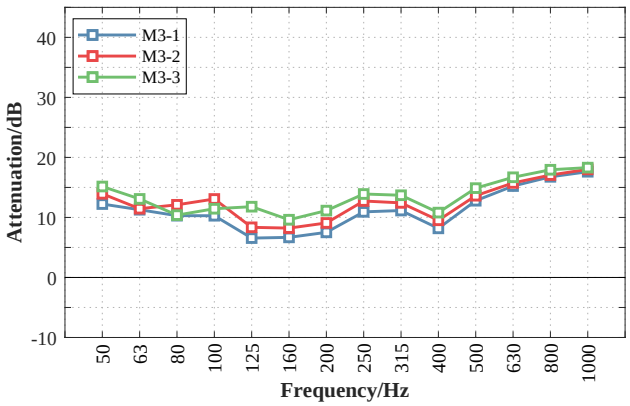

(c) twelve-point source

Figure 17: Predicted attenuations for the source to receiver distance of 20 meters

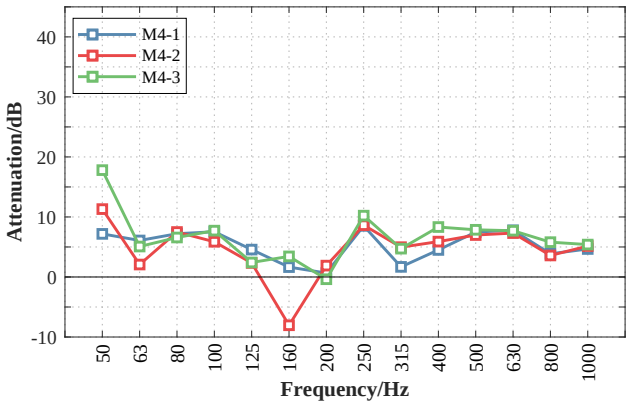

(a) one-point source

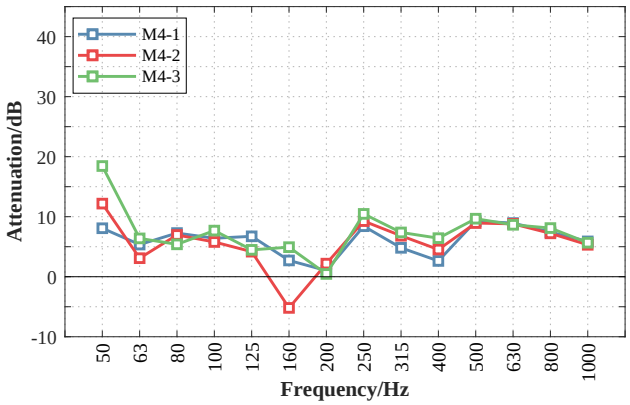

(b) four-point source

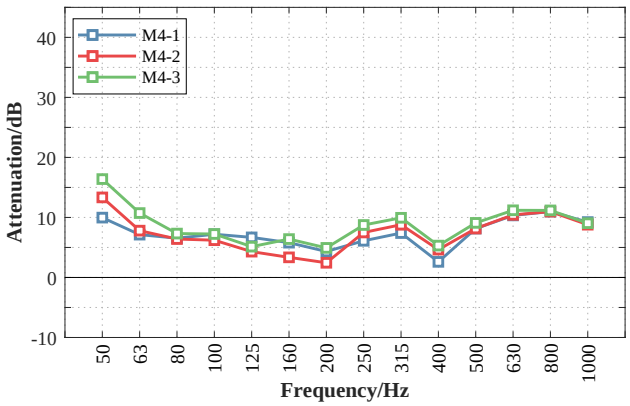

(c) twelve-point source

Figure 18: Predicted attenuations for the source to receiver distance of 40 meters